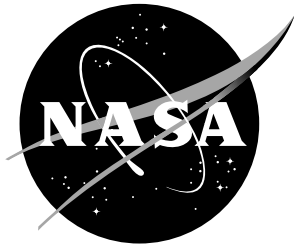


NASA/TM-2019-220275



An Analytical Method to Calculate Effective Elastic Properties of General Multifunctional Honeycomb Cores in Sandwich Composites

*Erik Sather and Thiagaraja Krishnamurthy
Langley Research Center, Hampton, Virginia*

April 2019

NASA STI Program... in Profile

Since its founding, NASA has been dedicated to the advancement of aeronautics and space science. The NASA scientific and technical information (STI) program plays a key part in helping NASA maintain this important role.

The NASA STI Program operates under the auspices of the Agency Chief Information Officer. It collects, organizes, provides for archiving, and disseminates NASA's STI. The NASA STI Program provides access to the NASA Aeronautics and Space Database and its public interface, the NASA Technical Report Server, thus providing one of the largest collection of aeronautical and space science STI in the world. Results are published in both non-NASA channels and by NASA in the NASA STI Report Series, which includes the following report types:

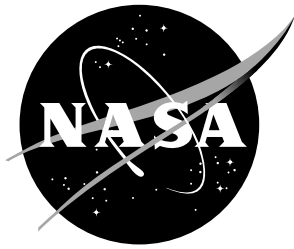
- **TECHNICAL PUBLICATION.** Reports of completed research or a major significant phase of research that present the results of NASA programs and include extensive data or theoretical analysis. Includes compilations of significant scientific and technical data and information deemed to be of continuing reference value. NASA counterpart of peer-reviewed formal professional papers, but having less stringent limitations on manuscript length and extent of graphic presentations.
- **TECHNICAL MEMORANDUM.** Scientific and technical findings that are preliminary or of specialized interest, e.g., quick release reports, working papers, and bibliographies that contain minimal annotation. Does not contain extensive analysis.
- **CONTRACTOR REPORT.** Scientific and technical findings by NASA-sponsored contractors and grantees.
- **CONFERENCE PUBLICATION.** Collected papers from scientific and technical conferences, symposia, seminars, or other meetings sponsored or co-sponsored by NASA.
- **SPECIAL PUBLICATION.** Scientific, technical, or historical information from NASA programs, projects, and missions, often concerned with subjects having substantial public interest.
- **TECHNICAL TRANSLATION.** English-language translations of foreign scientific and technical material pertinent to NASA's mission.

Specialized services also include organizing and publishing research results, distributing specialized research announcements and feeds, providing information desk and personal search support, and enabling data exchange services.

For more information about the NASA STI Program, see the following:

- Access the NASA STI program home page at <http://www.sti.nasa.gov>
- E-mail your question to help@sti.nasa.gov
- Phone the NASA STI Information Desk at 757-864-9658
- Write to:
NASA STI Information Desk
Mail Stop 148
NASA Langley Research Center
Hampton, VA 23681-2199

NASA/TM-2019-220275



An Analytical Method to Calculate Effective Elastic Properties of General Multifunctional Honeycomb Cores in Sandwich Composites

*Erik Saether and Thiagarajan Krishnamurthy
Langley Research Center, Hampton, Virginia*

National Aeronautics and
Space Administration

Langley Research Center
Hampton, Virginia 23681-2199

April 2019

The use of trademarks or names of manufacturers in this report is for accurate reporting and does not constitute an official endorsement, either expressed or implied, of such products or manufacturers by the National Aeronautics and Space Administration.

Available from:

NASA STI Program / Mail Stop 148
NASA Langley Research Center
Hampton, VA 23681-2199
Fax: 757-864-6500

Table of Contents

Abstract	1
1. Introduction	1
2. The unit cell approach for a honeycomb core structure	5
3. Analytical expressions for effective material properties of honeycomb structures	6
4. FEM analysis of a unit cell	8
4.1 In-plane analysis of a unit cell using a 1-D beam model	9
4.2 In-plane analysis of a unit cell honeycomb structure with 2-D shell elements	10
4.3 In-plane analysis of a unit cell honeycomb structure with 3-D solid elements	11
4.4 General 3-D analysis of a unit cell for a complete set of elastic moduli	12
5. Equivalent isotropic single layer material properties to represent a multi-layered honeycomb wall	14
6. Comparison of equivalent single layer isotropic properties for layered honeycomb structures using a finite element analysis of a unit cell.....	16
7. Reference solution for sandwich honeycomb structures with layered core-walls	21
8. Homogenized finite element models used to assess effective core properties	22
9. Comparison of maximum center deflection with reference solutions	24
9.1 Deflection comparison of a three-layered isotropic [Nomex/Nomex/Nomex] Laminate-1 core in a Sandwich plate with reference and homogenized solutions	24
9.2 Deflection comparison of a symmetric three-layer isotropic [Al/Cu/Al] Laminate-2 core in a sandwich plate with reference and homogenized solutions	25
9.3 Deflection comparison of an unsymmetrical three-layer isotropic [Al/Epoxy/Cu] Laminate-3 core in a sandwich plate with reference and homogenized solutions	25
10. Summary	27
11. References.....	28

Abstract

Sandwich composite structures are ideal configurations in which to incorporate additional functionality beyond load carrying capabilities. The inner core-walls can be layered to incorporate other functions such as power storage for a battery. In this work we investigate an assemblage of analytical tools to compute effective properties that allow complex layered core architectures to be homogenized into a single continuum layer. This provides a great increase in computational efficiency to numerically simulate the structural response of multifunctional sandwich structures under applied loads. We present a coupled analytical method including an extensive numerical verification of the accuracy of this method.

1. Introduction

Multifunctional structures seek to maximize operational efficiency by using materials that can perform several functions simultaneously. Sandwich composites are ideally suited for incorporating additional functions beyond load carrying capabilities. These composite structures are composed of two faceplates separated by a core material to increase bending stiffness and provide a light, stiff structure. A representative honeycomb core geometry is shown in Figure 1 and a depiction of a sandwich structure showing the attached faceplates in Figure 2.

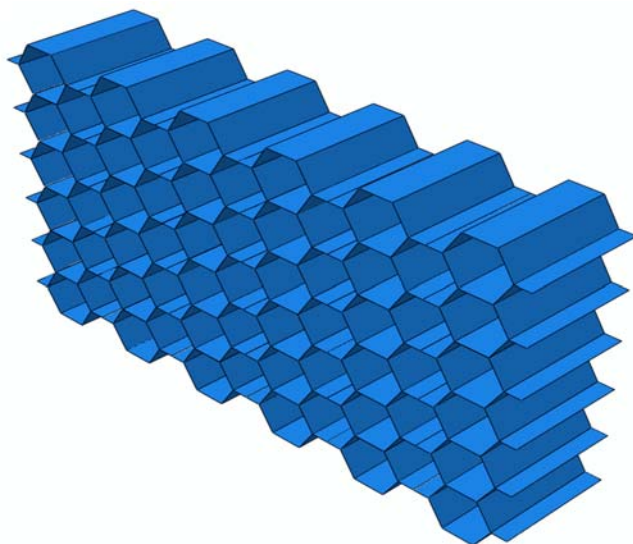


Figure 1. A representative honeycomb core configuration.

Various multifunctional applications for composites have been discussed in the literature, such as piezoelectric actuators, self-healing, sensing, and battery functions [1-4]. In this study, we will focus on potential core functionality as a battery. Structural battery materials are those that can carry mechanical loads while also storing electrical energy. Because these core geometries possess an open architecture of repeating cells, the cell walls can be layered with a suitable choice of materials to function as electrodes and electrolytes as required in a battery. The general battery configuration and the scope of the analysis performed in the present investigation was developed

in the NASA project entitled Multifunctional Structures for High Energy Lightweight Load-bearing Storage (M-Shells) [5].

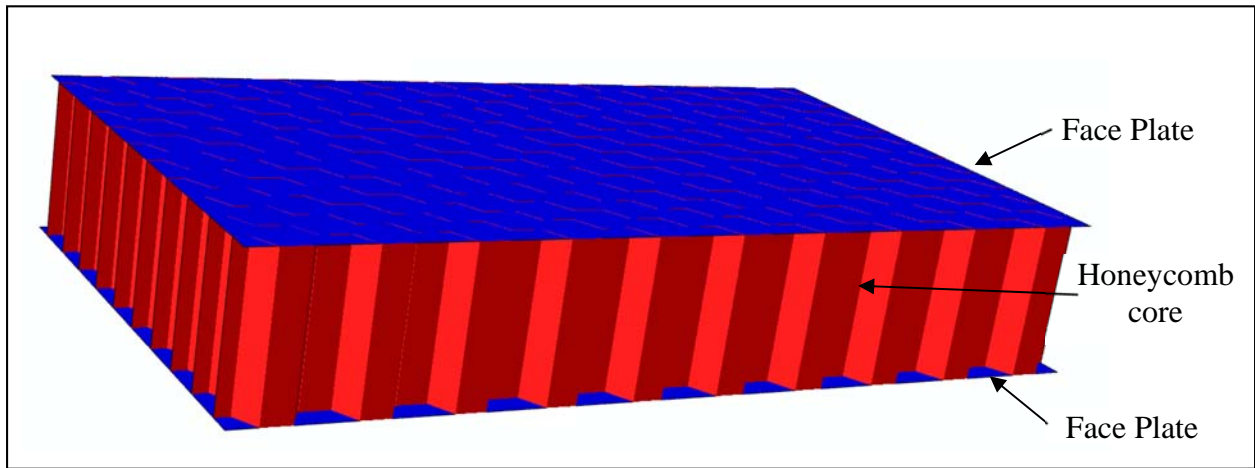


Figure 2. A schematic of a typical sandwich structure.

A core is typically configured as an array of cells which can assume many different geometrical architectures such as circular or polygonal cross sections [6]. Here we will focus on hexagonal honeycomb configurations that are sized to maintain a large bending stiffness in the sandwich panel. These cores are additionally assumed to include battery functionality. Figure 3 shows the idealized battery as a three-layer configuration with electrodes and electrolyte incorporated into the walls of the honeycomb.

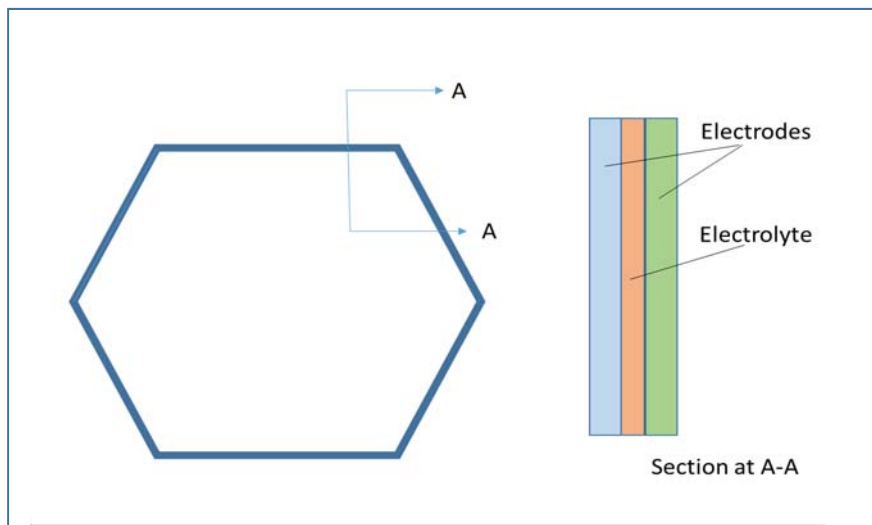


Figure 3. Walls of a honeycomb serving as a battery with materials that can function as electrodes and electrolyte.

Composite structures are typically analyzed using the finite element method (FEM). Composite sandwich structures, however, present a modeling challenge because they consist of a core region composed of a large number of cells that also have a complex geometry. While certain analyses - such as simulating sequential failure propagation within the core - would require a detailed finite element modeling of a small representative region of the core to determine the material response in damage propagation, other simulations of sandwich composite behavior involving a complete panel would require modeling a large number of core cells making an explicit simulation computationally expensive. Therefore, some homogenization method is needed to replace the core with a simplified solid layer with effective (equivalent) material properties. Many research efforts have been published that present various analytical methods for determining effective mechanical properties of homogenized core geometries that can avoid explicit modeling of the honeycomb geometry [7-11]. In general, the effective material properties for honeycomb structures are obtained from analyzing a unit cell representing a repeating element in a honeycomb structure. The most prevalent unit cell model for effective property determination is the 1-D isotropic beam analysis approach of Gibson et al. [7]. Gibson assumes that the linear-elastic response of the honeycomb deformations and resulting core properties depend only on bending of the core cell walls. Other deformation modes have been investigated that include stretching and shear deformation of the cell walls [8]. Many other approaches have been published [6] to estimate the effective material properties of honeycomb structures using the finite element method. For multifunctional honeycomb sandwich structures with built in battery functionality, it is necessary to compute equivalent elastic properties of core-walls composed of an arbitrary number of layers possessing different material properties. In particular, the electrolyte layers can have moduli that are orders of magnitude less than the materials used for the electrodes. There is a need to develop analytical expressions to predict the homogenized effective material properties for multifunctional honeycomb sandwich cores. These analytical expressions can then be used for rapid prototyping of multifunctional sandwich composites during the design phase to size the core for the intended service loads and for projected energy requirements.

Figure 4 illustrates the homogenization approach undertaken in this work. This approach is performed in two steps: (1) determine a single effective modulus for the multi-layered wall used in the core; and (2), use Gibson's approach to obtain equivalent elastic properties of the full core configurations such that they can be used in a uniform solid material representation. The homogenized core is then utilized to simplify finite element modeling of a sandwich core. This procedure is depicted in Figure 5.

Thus, the two objectives sought in this investigation are, first, to enhance the Gibson analysis by extending it to multi-layered isotropic walls, and second, to validate the methodology by comparing the analytical results with reference FEM simulations in which the multi-layered honeycomb geometry is explicitly modeled. All analyses are assumed to involve small deformations and exhibit an exclusively linear elastic response.

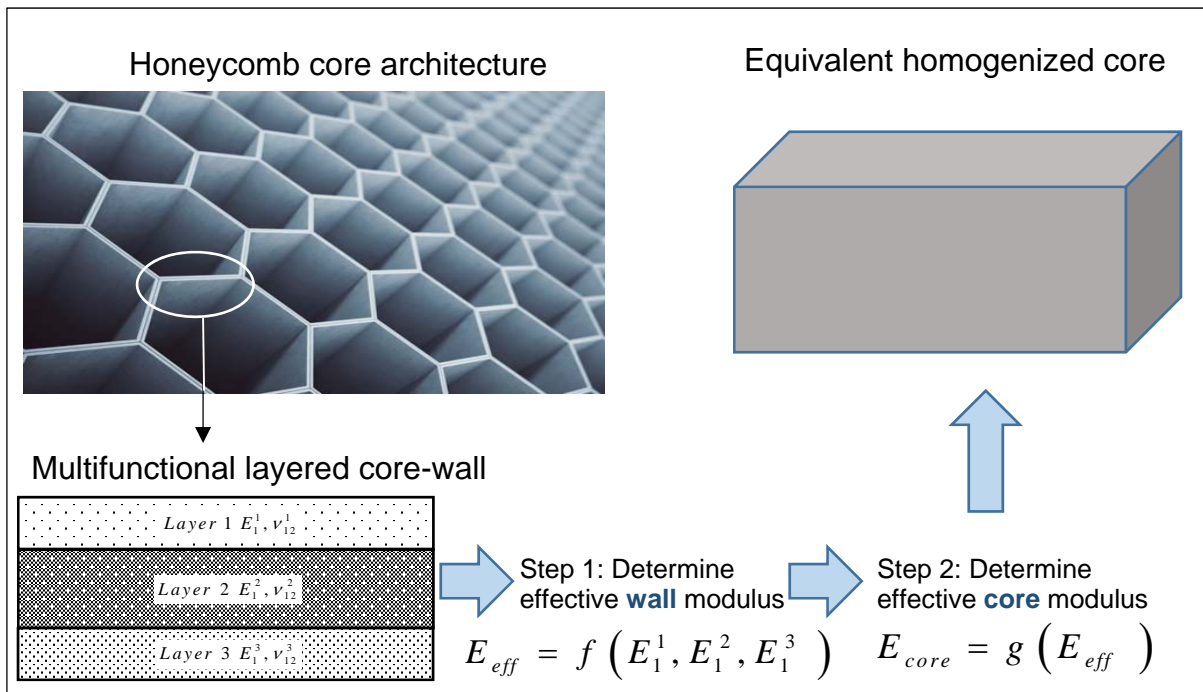


Figure 4. Overview of homogenization methodology sought in the current investigation.

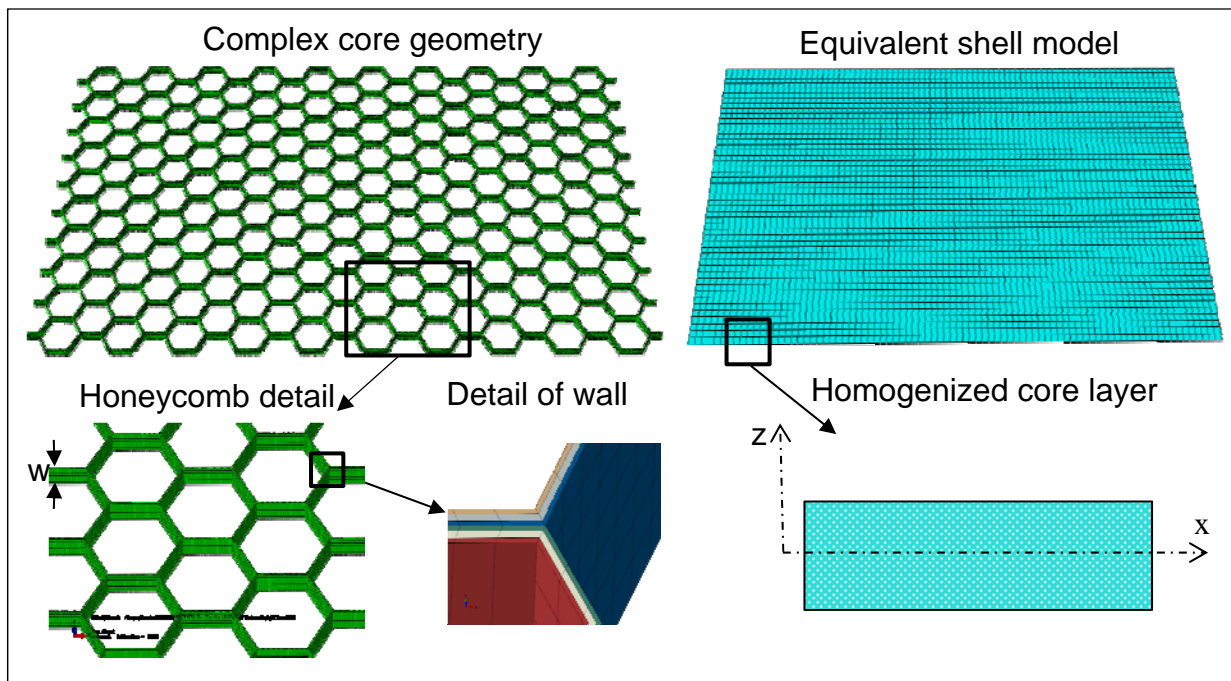


Figure 5. Simplified modeling of complex core geometry.

This report is organized into several sections: Section 2 defines unit cell models for the honeycomb structure used in the present investigation. Next, in Section 3, Gibson's analytical solutions for the effective in-plane elastic core properties are presented. In Section 4, the validity of the analytical approach is examined by using 1-D, 2-D, and 3-D finite element simulations to predict the elastic properties. The calculation of an equivalent modulus for multi-layered core-walls is contained in Section 5. This equivalent modulus will be used in the Gibson equations to simulate the elastic behavior of core-walls that are representative of multifunctional battery construction. In Section 6, various layer configurations are identified and the enhanced Gibson equations are used to compute effective moduli of the core. These moduli are validated by comparing them to elastic properties computed through unit cell finite element simulations. This is followed, in Section 7, by the development of reference solutions for several sandwich composite configurations with different layered cores. Homogenized 2-D shell and 3-D solid element models are developed in Section 8 to illustrate the use and accuracy of homogenizing sandwich cores that allow simplified finite element models to be used for rapid simulations. These models incorporate the derived effective core properties and, in Section 9, their maximum center deflection is compared to the reference solutions to verify the overall procedure for modeling multifunctional sandwich composite structures. Finally, a discussion is presented in Section 10 that focuses on the major issues examined in this report.

2. The unit cell approach for a honeycomb core structure

The effective homogenized material properties for a honeycomb structure are derived from analyzing the unit cell (repeating element) of the honeycomb. The geometry of the unit cell depends upon the method used to fabricate the honeycomb core. In this report, the honeycomb structure is assumed to be constructed from corrugated sheet-based technology [6]. The corrugated sheets are joined together by an adhesive to form the honeycomb geometry. The thin layer of adhesive material bonding the cells walls is considered to add negligible stiffness. In addition, the adhesive used in the manufacturing process can produce fillets where the honeycomb walls join, but the influence of a fillet on stiffness of the unit cell representation is assumed to have only a second order contribution and is neglected. However, with other geometries, the effect of fillet radius can be important in the failure modes exhibited by core cell structures under applied loads [6] and will be addressed in future work. In addition, at the interface at which the core is bonded to the faceplates, various fillets or adhesive layers can be formed but are assumed to be of secondary influence compared to the large stiffness of the faceplates [11].

The unit cell selected for this study is shown in Figures 6 and 7. The cell size (d), angle (θ), thickness (t) and width (w) completely define any honeycomb geometry of the unit cell. The length of the sides of the hexagonal honeycomb core (L) can be determined from d and θ as shown in Figure 6. For a regular hexagonal honeycomb structure, the angle θ equals 30 degrees.

The definition of the width, w , of the honeycomb geometry is shown in Figure 7. The width of the unit cells represents the separation of the faceplates.

$$E_{xx} = \frac{E_c \left(\frac{t}{L}\right)^3 \text{Cos}(\theta)}{(1 + \text{Sin}(\theta)) \text{Sin}^2(\theta)} \quad (1)$$

$$E_{yy} = \frac{E_c \left(\frac{t}{L}\right)^3 (1 + \text{Sin}(\theta))}{\text{Cos}^3(\theta)} \quad (2)$$

$$\nu_{xy} = \frac{\text{Cos}^2(\theta)}{(1 + \text{Sin}(\theta)) \text{Sin}(\theta)} \quad (3)$$

$$G_{xy} = E_c \left(\frac{t}{L}\right)^3 \frac{1 + \text{Sin}(\theta)}{3 \text{Cos}(\theta)} \quad (4)$$

where E_c is the elastic modulus of the wall. The out-of-plane elastic properties derived using Gibson's assumptions are presented in Reference [12] and are represented by

$$E_{zz} = \frac{\rho}{\rho_c} E_c \quad (5)$$

where ρ/ρ_c is the relative density of the equivalent core and

$$\nu_{xz} = \nu_c \frac{E_{xx}}{E_{zz}} \quad (6)$$

$$\nu_{yz} = \nu_c \frac{E_{yy}}{E_{zz}} \quad (7)$$

$$G_{xz} = G_{yz} = G_c \left(\frac{t}{L}\right) \frac{\text{Cos}(\theta)}{(1 + \text{Sin}(\theta))} \quad (8)$$

where ν_c and G_c are the Poisson's ratio and shear modulus of the wall. The Gibson's Equations (1) - (8) are valid only for a uniformly isotropic wall material.

Constraint effects on the effective in situ core properties are an important consideration. At the boundary where the core cells are bonded to the face plates, bending in the honeycomb cells is constrained and the core deformation is limited to the stretching of the face plates. Effective in-plane moduli for core deformation solely due to cell wall stretching modes, as shown in Figure 8, have been derived by Masters and Evans [8] and are given by Equations 9 – 12 for the in-plane properties. This effect would be expected to diminish within a region extending out from this interface. In this region the effective core moduli should transition from stretching-dominated elastic properties to bending-dominated elastic properties. Assuming a wall modulus, E_c , of unity, Table 1 shows a comparison of calculated effective moduli considering separately bending or stretching deformation modes for t/L ratios between 0.01 and 0.1. The lower magnitude modulus in bending indicates a naturally preferred deformation mode from an energy standpoint. Constraining the honeycomb cell to only deform through stretching can have a large effect on the

local core properties, and various aspects of this effect have been investigated in References [18] and [19]. For the remainder of this report, all deformations of the core cells are assumed to be unconstrained and consist only of bending in the core walls; however, a study of the effect of deformation mode transitioning on in situ core properties is planned for future work.

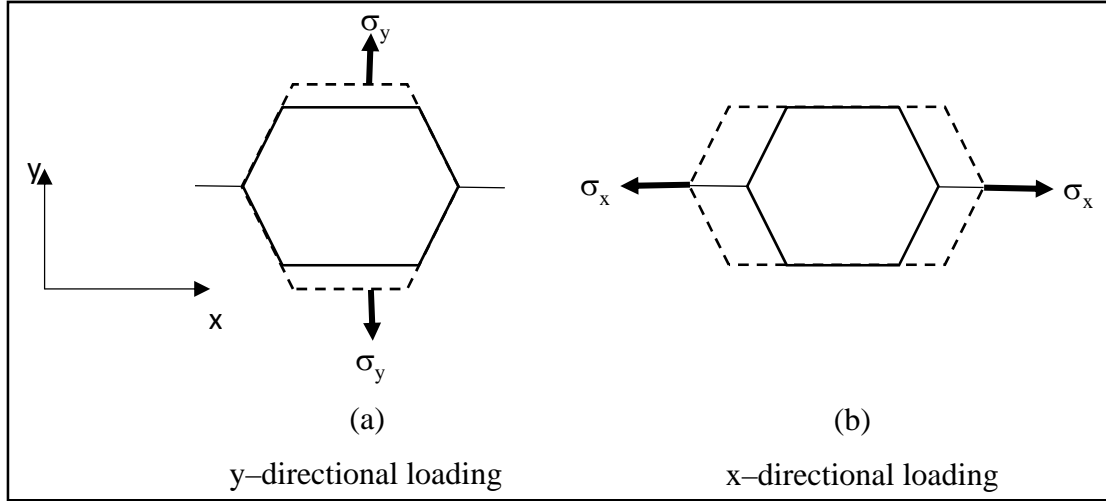


Figure 8. Stretching modes in a honeycomb core unit cell.

$$E_{xx} = \left(\frac{tE_c}{L} \right) \frac{(1 + \sin(\theta))}{\cos(\theta)(2 + \sin^2(\theta))} \quad (9)$$

$$E_{yy} = \left(\frac{tE_c}{L} \right) \frac{1}{\cos(\theta)(1 + \sin(\theta))} \quad (10)$$

$$G_{xy} = \left(\frac{E_c t}{L} \right) \frac{\cos(\theta)(1 + \sin(\theta))}{(\cos(\theta) + (1 + \sin(\theta))\sin(\theta))^2} \quad (11)$$

$$\nu_{xy} = - \frac{\sin(\theta)(1 + \sin(\theta))}{2 + \sin^2(\theta)} \quad (12)$$

Table 1. Comparison of effective moduli due to flexural (Gibson) and stretching (Masters) deformations.

t/L	Flexural E_{xx}, E_{yy}	Stretching E_{xx}, E_{yy}
0.010	2.31E-6	7.70E-3
0.033	7.94E-5	2.50E-2
0.055	3.84E-4	4.23E-2
0.078	1.07E-3	5.97E-2
0.100	2.31E-3	7.70E-2

4. FEM analysis of a unit cell

Numerical simulations of the hexagonal unit cell for the honeycomb core were performed using FEM with appropriate periodic boundary conditions. The FEM solution simulates all pertinent deformation modes including bending, stretching and shear, and is a reference solution for the analytical Gibson solution which assumes only bending deformations. The Gibson formula for the in-plane moduli is independent of the core width. To evaluate the assumptions of the Gibson analysis, three different models were analyzed to account for 1-D, 2-D and 3-D stress states in the walls of the unit cell. These models are:

- (a) 1-D beam model
- (b) 2-D shell model
- (c) 3-D solid model

The results from these studies are compared with the analytical results of Gibson et al. [7] which are based solely on the 1-D elasticity of beam bending. Linear elastic isotropic properties were used with $t = 0.052$ mm, $E_c = 3150$ MPa, $G_c = 1125$ MPa and $\nu_c = 0.4$ as used in Reference [18]. With these values, Gibson's formula predicts the in-plane moduli of the core to be: $E_{xx} = E_{yy} = 0.04806$ MPa.

4.1 In-plane analysis of a unit cell using a 1-D beam model

The unit cell beam model shown in Figure 9 was analyzed using ABAQUS [16] with B21 linear beam elements. The width was fixed at 1.0 mm and the effective in-plane moduli E_{xx} and E_{yy} were calculated. In this model, the cell width effects the moment of inertia of the cross section but cannot alter the 1-D stress state. The results from FEM unit cell analysis are compared with analytical results from Gibson in Table 2. The beam FEM model predicts effective properties within one percent of Gibson's analytical model and shows that any axial deformation is negligible.

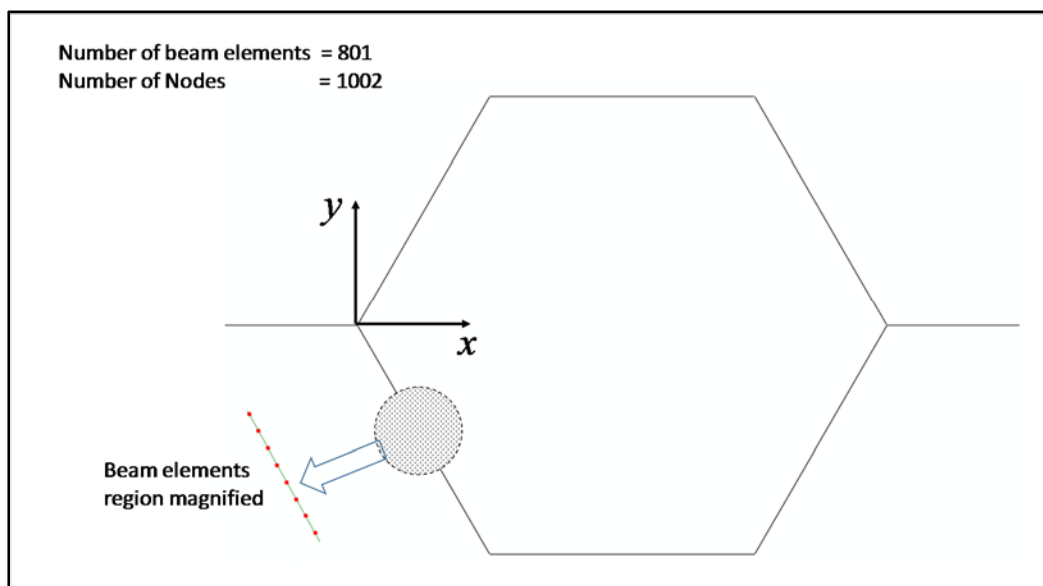


Figure 9. Unit cell beam FEM model

Table 2. Effective core moduli for a beam model: Comparison of Gibson ($E_{xx} = E_{yy} = 0.04806$ MPa) and numerical FEM results.

E_{xx} (MPa)		E_{yy} (MPa)	
FEM	% difference of Gibson solution from FEM	FEM	% difference of Gibson solution from FEM
0.0476	0.96	0.0477	0.96

4.2 In-plane analysis of a unit cell honeycomb structure with 2-D shell elements

The FEM for the unit-cell shell model is shown in Figure 10. The shell model was analyzed for different honeycomb widths ranging from 0.125 mm to 10 mm. Simulations were performed using ABAQUS with 4-node S4R reduced integration shell elements. The results from FEM analyses are compared with the analytical solution of Gibson [7] in Table 3. For widths greater than 5 mm, the maximum difference between the FEM and the Gibson's analytical solution is around 15 percent, indicating a departure of a 1-D beam solution from a 2-D stress state obtained using shell elements. With increasing width, this maximum difference is approached asymptotically and, therefore, is bounded.

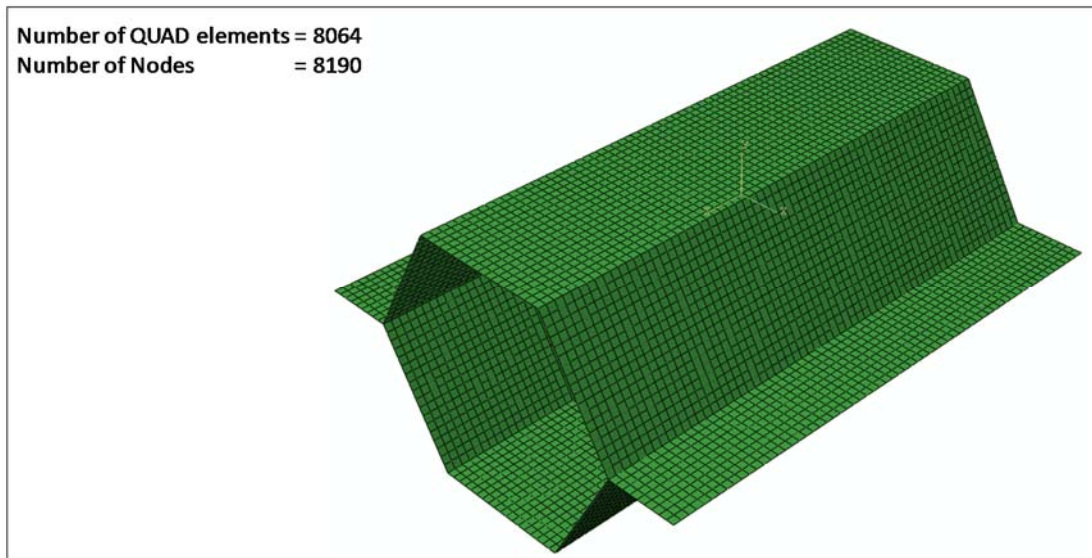


Figure 10. Unit cell shell FEM model

Table 3. Effective core moduli for a shell model: Comparison of Gibson ($E_{xx} = E_{yy} = 0.04806$ MPa) and numerical FEM results.

Width Mm	E_{xx} (MPa)		E_{yy} (MPa)	
	FEM	% difference of Gibson solution from FEM	FEM	% difference of Gibson solution from FEM
0.125	0.0477	0.6	0.0477	0.6
0.25	0.0478	0.6	0.0478	0.6
0.5	0.0491	2.2	0.0491	2.2
1	0.0513	6.7	0.0512	6.6
5	0.0546	14.0	0.0546	14.0
10	0.0550	15.0	0.0550	15.0

4.3 In-plane analysis of a unit cell honeycomb structure with 3-D solid elements

The unit cell model was analyzed using ABAQUS 8-node solid continuum elements and is shown in Figure 11. The ABAQUS C3D8I element incorporates incompatible modes and full integration. Solid elements can represent a complete 3-D state of stress which was not expected in these simulations due to the small thickness-to-length ratio of the honeycomb walls. Here a similar parametric study as made in Section 4.2 was performed with the widths of the unit cell model varied from 0.125 mm to 10 mm.

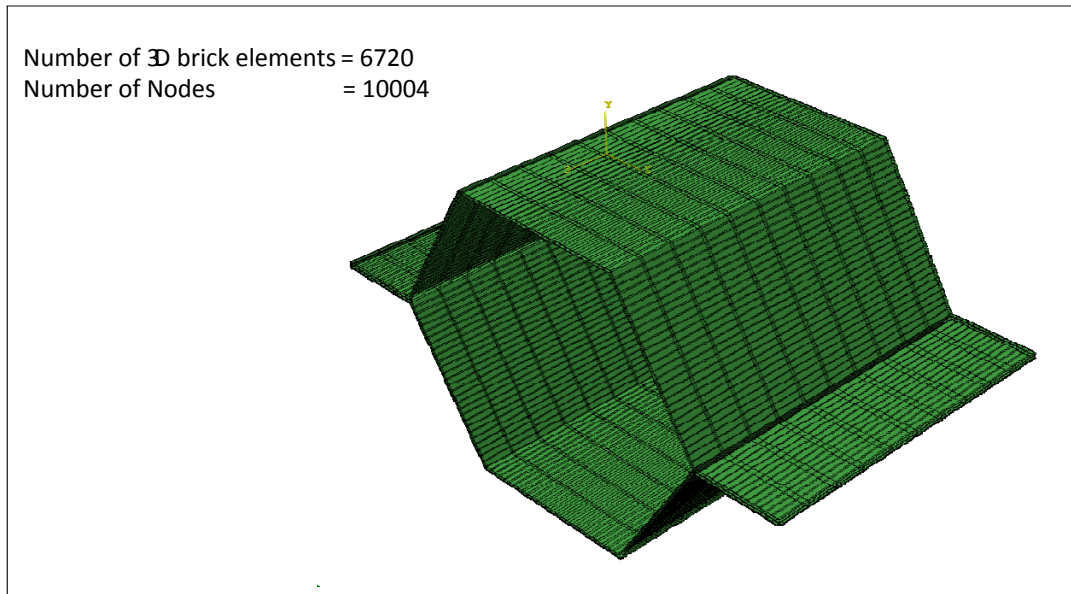


Figure 11. Unit cell 3-D solid FEM model.

The 3-D elastic solid elements prediction of effective moduli are compared with Gibson's analytical predictions in Table 4. For widths greater than 5 mm, the difference between the FEM and the Gibson's analytical solutions asymptotically approach approximately 18 percent.

Table 4. Comparison of Gibson ($E_{xx} = E_{yy} = 0.04806$ MPa) and numerical results for effective core moduli using a solid FEM model.

Width (mm)	E_{xx} (MPa)		E_{yy} (MPa)	
	FEM	% difference of Gibson solution from FEM	FEM	% difference of Gibson solution from FEM
0.125	0.0484	1.0	0.0483	1.0
0.25	0.0498	3.8	0.0496	3.3
0.5	0.0526	9.6	0.0519	8.0
1	0.0547	14.0	0.0540	13.0
5	0.0566	18.0	0.0558	16.0
10	0.0568	18.0	0.0561	17.0

From the analyses using both 2-D shell and 3-D solid models, it is clear that the unit-cell FEM model predicts the effective modulus of the material to agree with Gibson's analysis for small widths but asymptotically increases to an 18 percent difference for larger widths. A comparison of results from the shell and solid element models indicates that 2-D shell elements are sufficient to represent the stress state of honeycomb cores. This will be further corroborated in Section 8 where cores with different layer properties are investigated.

4.4 General 3-D analysis of a unit cell for a complete set of elastic moduli

A final set of computations was performed to obtain the six in-plane and out-of-plane moduli of a unit cell model with various cell widths. These equivalent moduli are presented in Table 5. When the calculated Gibson values for these moduli are normalized by the FEM predictions, the normalized moduli for E_{xx} and E_{yy} , and for E_{zz} and G_{yz} follow the same curve and have been perturbed slightly to be visible in Figure 12.

Table 5. Complete set of equivalent elastic moduli of a honeycomb core as a function of cell width, w .

Elastic Component	Numerical FEM, $w =$					Analytical Gibson
	0.125 mm	0.25 mm	2.00 mm	14.0 mm	24.0 mm	
E_{xx} (MPa)	0.04899	0.04831	0.0532	0.0552	0.0553	0.0481
E_{yy} (MPa)	0.04899	0.04831	0.0532	0.0552	0.0553	0.0481
E_{zz} (MPa)	91.0000	90.9727	91.013	91.003	90.003	91.000
G_{xy} (MPa)	0.01493	0.01576	0.0175	0.0173	0.0173	0.0120
G_{xz} (MPa)	10.564	10.565	10.564	10.564	10.563	12.188
G_{yz} (MPa)	12.205	12.205	12.205	12.199	12.197	12.188

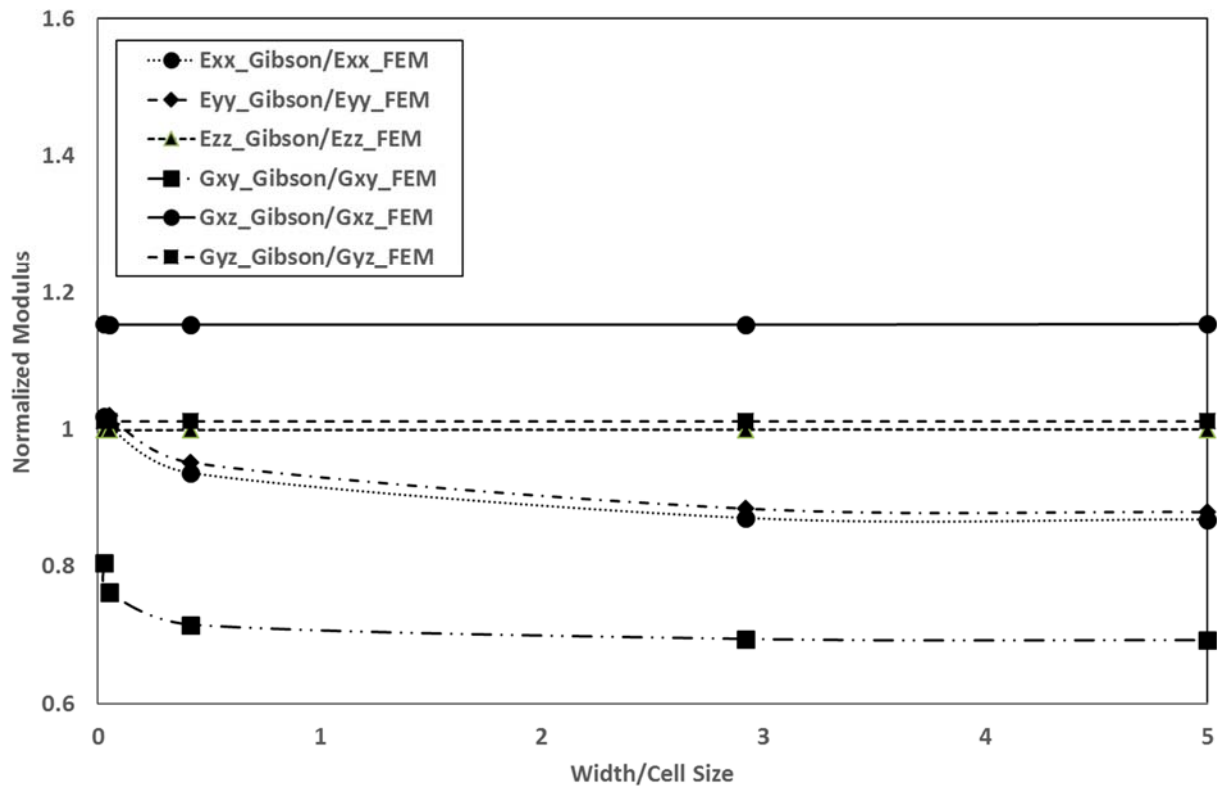


Figure 12. The six in-plane and out-of-plane elastic moduli for a unit hexagonal core cell.

In Figure 12, the in-plane moduli, E_{xx} , E_{yy} and G_{xy} , show a dependence on cell width when the width becomes lower than 15.0. This is presumed to be due to the stress state transitioning from a 1-D beam bending stress state to a 2-D stress state. This is corroborated by the results in Tables 3 and 4 that show an asymptotic convergence to in-plane moduli after a core width of approximately 5 mm. The other out-of-plane elastic moduli appear to be relatively independent of the cell width and are effectively constant for the dimensions investigated.

5. Equivalent isotropic single layer material properties to represent a multi-layered honeycomb wall

In order to rapidly assess design variations and sizing requirements of configurations with multi-layered cell walls, the multi-layer wall must be replaced with a single equivalent isotropic layer. To store energy as a battery, the honeycomb walls consist of three distinct materials to function as an anode, a cathode, and an electrolyte. The modulus of the equivalent wall layer is then used within the analytical expressions derived by Gibson et al. [7] to allow multi-layered cores to be modeled as a simple homogeneous material. In this section, classical lamination theory (CLT) is used to compute equivalent single-layer in-plane elastic properties of the laminated walls.

For a multi-layered wall, effective in-plane properties can be computed via CLT using the laminate A, B and D matrices [13,14].

$$\begin{bmatrix} [A] & [B] \\ [B]^T & [D] \end{bmatrix} = \begin{bmatrix} A_{11} & A_{12} & A_{16} & B_{11} & B_{12} & B_{16} \\ A_{21} & A_{22} & A_{26} & B_{21} & B_{22} & B_{26} \\ A_{61} & A_{26} & A_{66} & B_{61} & B_{62} & B_{66} \\ \hline B_{11} & B_{21} & B_{61} & D_{11} & D_{12} & D_{16} \\ B_{12} & B_{22} & B_{62} & D_{21} & D_{22} & D_{26} \\ B_{16} & B_{26} & B_{66} & D_{61} & D_{62} & D_{66} \end{bmatrix} \quad (13)$$

where

$$A_{ij} = \sum_{k=1}^n (\bar{Q}_{ij})_k (z_k - z_{k-1}) \quad i, j = 1, 2, 6 \quad (14)$$

$$B_{ij} = \frac{1}{2} \sum_{k=1}^n (\bar{Q}_{ij})_k (z_k^2 - z_{k-1}^2) \quad i, j = 1, 2, 6 \quad (15)$$

$$D_{ij} = \frac{1}{3} \sum_{k=1}^n (\bar{Q}_{ij})_k (z_k^3 - z_{k-1}^3) \quad i, j = 1, 2, 6 \quad (16)$$

Where \bar{Q}_{ij} are the reduced stiffnesses of the k^{th} layer, z_k is the location of the layer interface through the thickness of the core-wall, and n is the number of layers in the laminate. The constitutive matrix relating strains and curvatures with force and moment resultants for the laminate is given by

$$\begin{Bmatrix} \varepsilon^o \\ \kappa \end{Bmatrix} = \begin{bmatrix} a & b \\ b^T & d \end{bmatrix} \begin{Bmatrix} N \\ M \end{Bmatrix} \quad (17)$$

where

$$\begin{bmatrix} a & b \\ b^T & d \end{bmatrix} = \begin{bmatrix} A & B \\ B^T & D \end{bmatrix}^{-1} \quad (18)$$

The equivalent in-plane material properties for a layered wall obtained by CLT are given by

$$\begin{aligned}
E_{xx} &= \frac{1}{a_{11}t} \\
E_{yy} &= \frac{1}{a_{22}t} \\
\nu_{xy} &= -\frac{a_{12}}{a_{11}} \\
G_{xy} &= \frac{1}{a_{66}t}
\end{aligned} \tag{19}$$

Chen and Chan [15] derive a set of modified in-plane moduli that account for induced shear and bending deformation in the equivalent single layer. These moduli are defined by elements of a P matrix defined as:

$$[P] = [a] - [b][d]^{-1}[b]^T \tag{20}$$

such that

$$\begin{aligned}
E_{xx} &= \frac{1}{\left(P_{11} - \frac{P_{16}^2}{P_{66}}\right)t} \\
E_{yy} &= \frac{1}{\left(P_{22} - \frac{P_{26}^2}{P_{66}}\right)t} \\
\nu_{xy} &= -\frac{P_{12} - \frac{P_{13}P_{26}}{P_{66}}}{P_{11} - \frac{P_{16}^2}{P_{66}}} \\
G_{xy} &= \frac{1}{\left[P_{66} - \frac{1}{\Delta_1} \left(P_{16}^2 P_{22} - 2P_{26}P_{16} + P_{26}^2 P_{11}\right)\right]t}
\end{aligned} \tag{21}$$

where

$$\Delta_1 = P_{11}P_{22} - P_{12}^2 \tag{22}$$

Averaged properties defined for an equivalent single layer using CLT in Equation (19) or by the Chen-Chan Equations (21) are then used in the Gibson Equations (1) through (8) to obtain the effective homogenized material properties of a honeycomb core possessing a layered wall. It should be noted that if the laminate is balanced such that the coupling B matrix is null, the Chen-Chan Equations and the CLT Equations yield identical results. The homogenized effective core properties obtained using Gibson's equations together with the averaged single layer properties are validated using a unit cell finite element analysis in the following section.

6. Comparison of equivalent single layer isotropic properties for layered honeycomb structures using a finite element analysis of a unit cell

The equivalent single layer properties defined using CLT Equations (19) or the modified Chen-Chan Equations (21) have to be verified before using Gibson's equations (1) to (8) to approximate the entire core. In this section, the equivalent single layer properties are validated using finite element analysis of a honeycomb unit cell. For finite element simulation, the single layer walls of the unit cell defined in Figures (6) and (7) are replaced by a three-layered laminate, as shown in Figure 13.

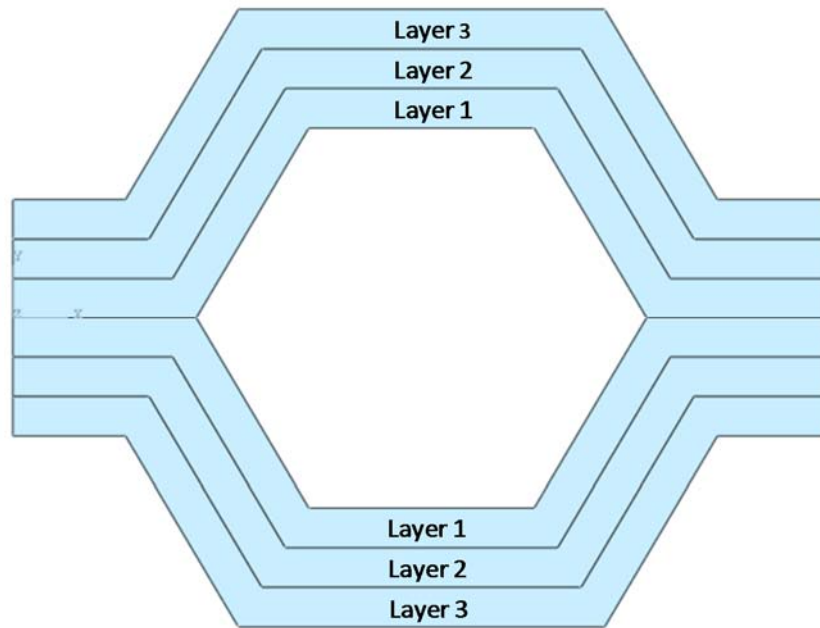


Figure 13. Honeycomb unit cell geometry with a three-layered laminated wall

Three different laminates were considered for the three-layered honeycomb wall. The lay-ups were selected to have an increasing difference in elastic moduli and to transition from a symmetric to an unbalanced laminate.

Laminate-1 consists of three isotropic layers with properties characteristic of lightweight Nomex core material. These properties are listed in Table 6.

Table 6. Laminate-1 multi-layer core-wall for [Nomex/Nomex/Nomex].

Layer	Thickness	Modulus	Poisson's Ratio
Nomex Paper	0.01733 mm	3150 MPa	0.40
Nomex Paper	0.01733 mm	3150 MPa	0.40
Nomex Paper	0.01733 mm	3150 MPa	0.40

Laminate-2 consists of aluminum and copper layers. The properties for Laminate-2 are given in Table 7.

Table 7. Laminate-2 multi-layer core-wall for [Al/Cu/Al].

Layer	Thickness	Modulus	Poisson's Ratio
Aluminum	0.01733 mm	70,300 MPa	0.330
Copper	0.01733 mm	110,000 MPa	0.343
Aluminum	0.01733 mm	70,300 MPa	0.330

Laminate-3 consists of Aluminum, Epoxy and Copper layers. The properties for Laminate-3 are given in Table 8. Laminate-3 is selected to represent realistic battery wall properties. The outer layers represent cathode and anode materials while the middle epoxy layer represents the separator to prevent contact between the electrodes.

Table 8. Laminate-3 multi-layer battery wall for [Al/Epoxy/Cu].

Layer	Thickness	Modulus	Poisson's Ratio
Aluminum	0.05 mm	70,300 MPa	0.330
Epoxy	0.20 mm	4237 MPa	0.450
Copper	0.05 mm	110,000 MPa	0.343

Laminate-1 and Laminate-2 possess a balanced assemblage of layers and the B matrix is identically zero. As stated above, this results in the CLT and Chen-Chan in-plane effective moduli being equal. However, for Laminate-3, the layer properties are not balanced and the computed wall modulus for the CLT and Chen-Chan in-plane moduli are different. The computed equivalent single layer isotropic wall moduli for the three laminates considered are given in Tables 9 to 11.

Table 9. Laminate-1: Equivalent single layer isotropic wall modulus

Effective Core Wall Properties	In-plane Moduli using CLT relations	In-plane Moduli using Chen-Chan relations
E_{xx}, E_{yy}	3150.0 MPa	3150.0 MPa
G_{xy}	1125.0 MPa	1125.0 MPa
ν_{xy}	0.4	0.4

Table 10. Laminate-2: Equivalent single layer isotropic wall modulus

Effective Core Wall Properties	In-plane Moduli using CLT relations	In-plane Moduli using Chen-Chan relations
E_{xx}, E_{yy}	83537.2 MPa	83537.2 MPa
G_{xy}	31270.0 MPa	31270.0 MPa
ν_{xy}	0.336	0.336

Table 11. Laminate-3: Equivalent single layer isotropic wall modulus

Effective Core Wall Properties	In-plane Moduli using CLT relations	In-plane Moduli using Chen-Chan relations
E_{xx}, E_{yy}	31,507.5 MPa	32,916.3 MPa
G_{xy}	11,698.6 MPa	12,204.3 MPa
ν_{xy}	0.347	0.349

The homogenized effective elastic properties for the unit cell are obtained using FEM analysis modeling the walls of the unit cell as a three-layered composite. The width of the modeled cell was 14.5 mm. The unit cell finite element model was created using 8064 4-node shell elements (S4R in ABAQUS) and 8193 nodes. For each of the 9 elastic constants a different set of loads and support conditions are applied to an FEM model and the response simulated. For example, the displacement boundary conditions applied to the unit cell to compute the effective in-plane E_{xx} and E_{yy} moduli are shown in Figure 14. In this approach, the strains are determined from the applied displacements divided by the model length in the x or y direction, and the stresses are obtained from the recovered reaction forces due to the imposed loading divided by the area over which the reaction forces are obtained. The 1-D moduli then become a simple calculation of the stress divided by the strain along these axes. A succinct enumeration of the boundary conditions used for each set of boundary conditions is contained in Reference 12 and are not elaborated here.

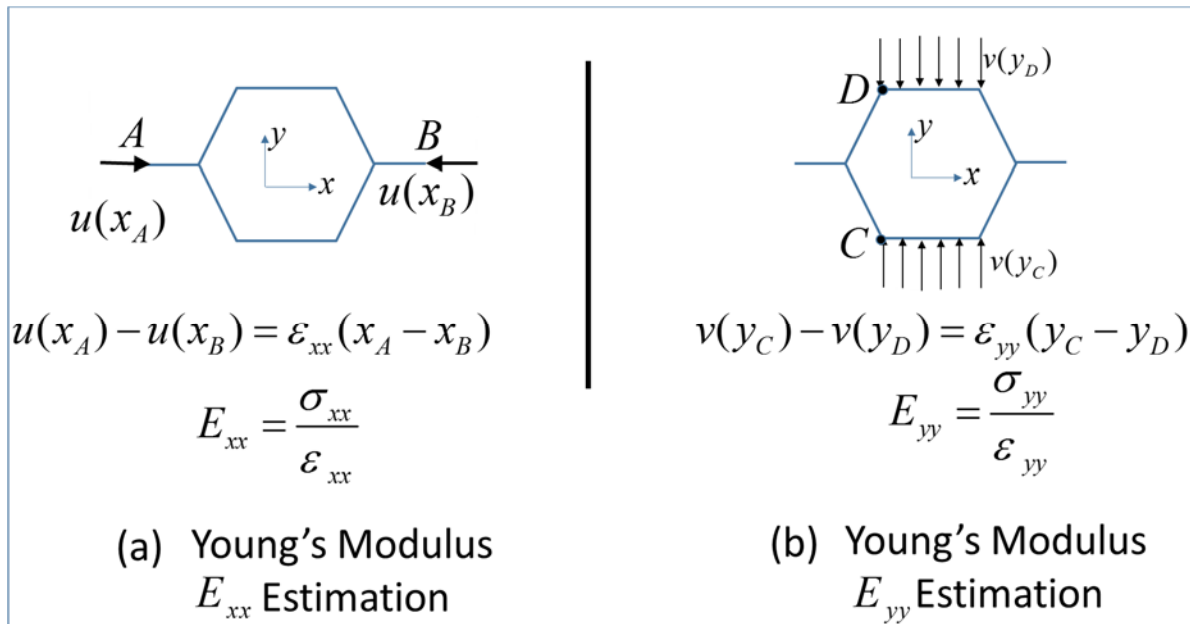


Figure 14. Applied displacements boundary conditions to impose unit cell strains

The estimated homogenized effective material properties for the unit cell from FEM simulations are compared with the calculated effective core elastic properties from the Gibson's equations (using conventional CLT and the Chen-Chan modified properties as presented in Section 5). Because the Chen-Chan equations are identical to the CLT equations for balanced laminates, only one set of results is shown for Laminate-1 and Laminate-2, whereas for Laminate-3, which is nonsymmetric, two separate tables are shown for these two sets of effective properties. These results are presented in Tables 12 - 15. The percent difference provides a measure of how well the effective wall properties used in Gibson's equations are representing the elastic response of the core-walls.

Table 12. Laminate-1: Effective honeycomb core elastic properties obtained from FEM and the Gibson equations modified using the Chen-Chan relations.

Property	FEM	Gibson	% Difference
E_{xx} MPa	0.05518	0.04806	12.90
E_{yy} MPa	0.05516	0.04806	12.87
E_{zz} MPa	91.00	91.00	0.0031
ν_{xy}	0.9985	1.00	-0.15
ν_{xz}	2.425E-4	2.112E-4	12.91
ν_{yz}	2.424E-4	2.112E-4	12.90
G_{xy} MPa	0.01680	0.01201	28.51
G_{xz} MPa	10.43	12.19	-16.87
G_{yz} MPa	12.20	12.19	0.082

Table 13. Laminate-2: Effective honeycomb core elastic properties obtained from FEM and the Gibson equations modified using the Chen-Chan relations.

Property	FEM	Gibson	% Difference
E_{xx} MPa	1.177	1.275	-8.32
E_{yy} MPa	1.194	1.275	-6.78
E_{zz} MPa	2413.0	2413.0	-0.0002
ν_{xy}	0.9994	1.00	-0.06
ν_{xz}	1.614E-4	1.748E-4	-8.30
ν_{yz}	1.637E-4	1.748E-4	-6.78
G_{xy} MPa	0.3928	0.3186	18.89
G_{xz} MPa	356.3	338.8	4.91
G_{yz} MPa	339.1	338.8E	0.09

Table 14. Laminate-3: Effective honeycomb core elastic properties obtained from FEM and the Gibson equations modified using the Chen-Chan relations.

Property	FEM	Gibson	% Difference
E_{xx} MPa	97.92	96.43	1.52
E_{yy} MPa	97.55	96.43	1.14
E_{zz} MPa	5466.0	5486.0	-0.35
ν_{xy}	0.9630	1.00	-3.84
ν_{xz}	6.253E-3	6.135E-3	1.88
ν_{yz}	6.229E-3	6.135E-3	1.49
G_{xy} MPa	26.35	24.11	8.44
G_{xz} MPa	816.7	762.8	6.60
G_{yz} MPa	757.8	762.8	-0.66

Table 15. Laminate-3: Effective honeycomb core elastic properties obtained from FEM and the Gibson equations modified using CLT approximations.

Property	FEM	Gibson	% Difference
E_{xx} MPa	97.92	92.31	5.73
E_{yy} MPa	97.55	92.31	5.37
E_{zz} MPa	5466.0	5251.0	3.93
ν_{xy}	0.9630	1.00	-3.80
ν_{xz}	6.253E-3	6.100E-3	2.44
ν_{yz}	6.229E-3	6.100E-3	2.07
G_{xy} MPa	26.35	23.08	12.41
G_{xz} MPa	816.7	731.2	10.47
G_{yz} MPa	757.8	731.2	3.51

The Gibson equations that are modified by the Chen-Chan approximations to obtain effective core properties presented in Tables 12 through 14, demonstrated a reasonably close agreement with the same quantities obtained through finite element simulations. It should be noted that, in Sections 4.2 and 4.3, it was shown that there is a departure of the Gibson results from the FEM predictions with increasing width of the cell due to the 1-D beam solutions not fully accounting for the 2-D stress state in deflections, and possibly due to deformation modes other than bending that are not included in Gibson's analysis. These modeling effects will influence the deviation of the elastic properties using Gibson's equations from the FEM predictions. In the three laminates examined, the least deviation is seen in the in-plane normal moduli which varied between 1.1% and 12.9%. The Poisson ratios showed a similar range of deviations for the different laminates, a trend that was also observed by Sorohan et al. [2]. In general, the shear moduli showed a larger deviation, which was also noted by Penado [17] in a study of effective moduli determination in which it was observed that a discrepancy in the calculation of the in-plane shear modulus, G_{xy} , could be explained by its relatively small magnitude compared to the out-of-plane shear moduli, which were 1-3 orders of magnitude greater and less susceptible to numerical precision issues.

7. Reference solution for sandwich honeycomb structures with layered core-walls

A high-fidelity FEM of a sandwich structure consisting of a 10 x 10 unit cell honeycomb core and two faceplates was developed as shown in Figure 15. The model contained a complete representation of the core architecture with multi-layered cell walls. The deflection response of this model under uniform pressure on the upper face plate provided reference solutions to compare with simulations using homogenized effective properties of the core. These homogenized cores simplify the finite element modeling which, in turn, minimize the computational cost and the overall simulation times.

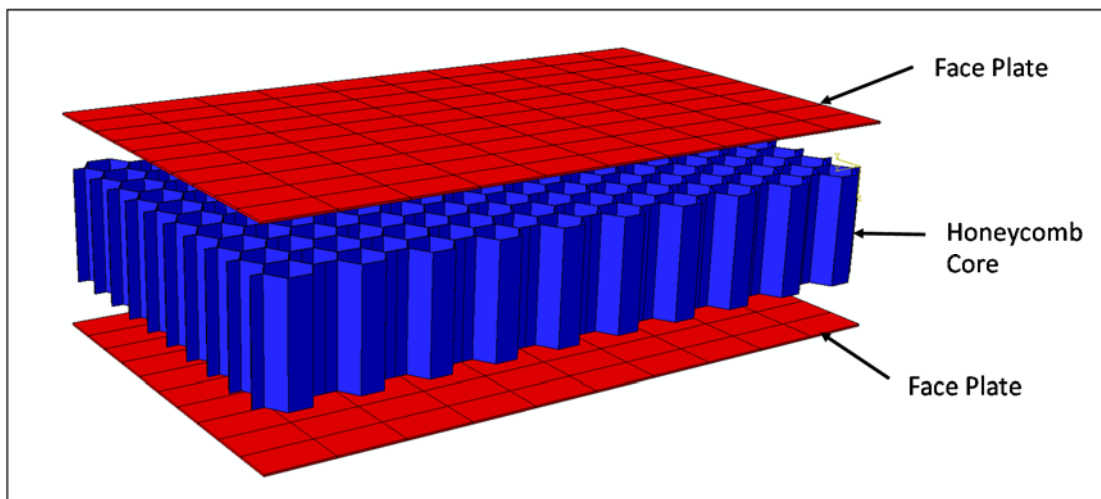


Figure 15. Sandwich composite configuration used to obtain the reference

Three reference solutions were generated with the three laminates described in Sections 5 and 6. The materials used for faceplates and the core for the three reference solutions are given in Table 16. Each model consists of 661,600 4-node S4R elements and 644,462 nodes.

Table 16. Materials and thickness of faceplates and cores used in the reference solutions.

Reference Solution	Lower Faceplate	Honeycomb Core	Upper Faceplate
1	Nomex, $w=0.25\text{mm}$	Laminate-1, $w=14.0\text{mm}$	Nomex, $w=0.25\text{mm}$
2	Steel, $w=0.25\text{mm}$	Laminate-2, $w=14.0\text{mm}$	Steel, $w=0.25\text{mm}$
3	Aluminum, $w=0.25\text{ mm}$	Laminate-3, $w=14.0\text{mm}$	Aluminum, $w=0.25\text{mm}$

The loading and boundary conditions are shown schematically in Figure 16. The nodes on the vertical faces that extend up from the outer edges of the model were assigned clamped boundary conditions, and a uniform normal pressure of 1.0 MPa was applied over the upper face.

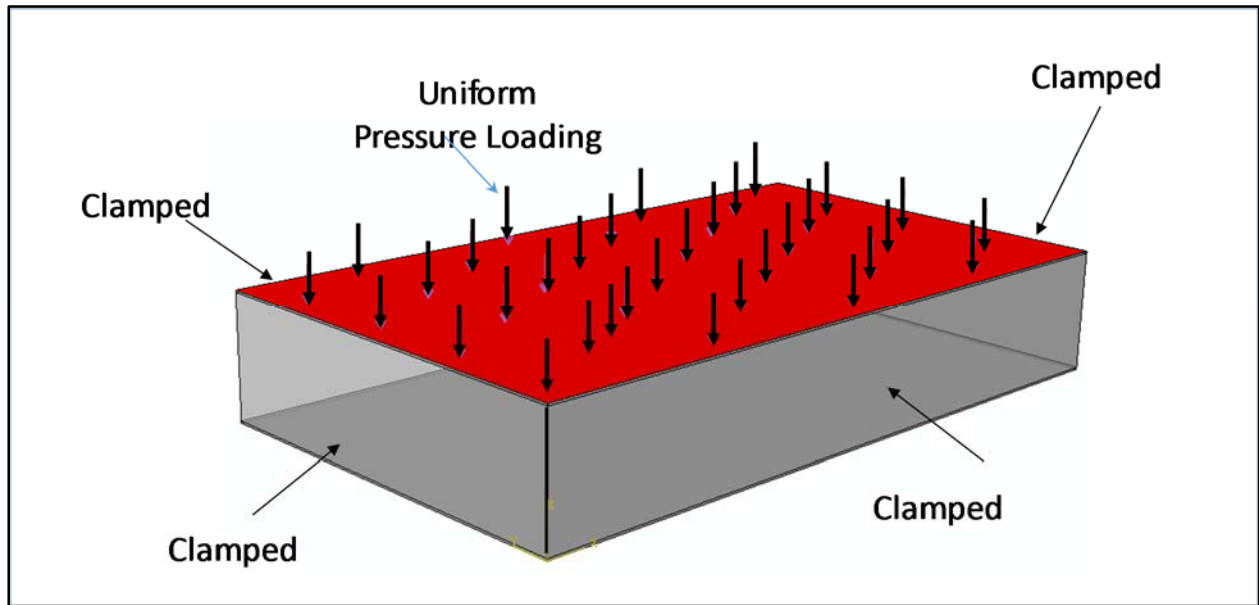


Figure 16. Schematic of applied surface loads and edge boundary conditions.

High fidelity finite element analyses of the three reference sandwich panels were performed. The maximum center deflection obtained from the analyses are given in Table 17.

Table 17. Maximum Center deflection for the three reference solutions

Reference Solution	Maximum center deflection (mm)
1	-1.4758
2	-.04594
3	-.02768

These reference solutions will be used to verify the center deflection of the homogenized models in the next section.

8. Homogenized finite element models used to assess effective core properties

A 2-D shell model and a 3-D solid model of the sandwich structure were created to assess the accuracy of replacing the honeycomb core configurations with an effective homogenized layer to improve computational efficiency. The shell model is composed of 7,104 4-node S4R elements and 7,280 nodes, while the solid model is composed of 478,080 8-node C3D8R elements and 502,169 nodes. These models are depicted in Figures 17 and 18.

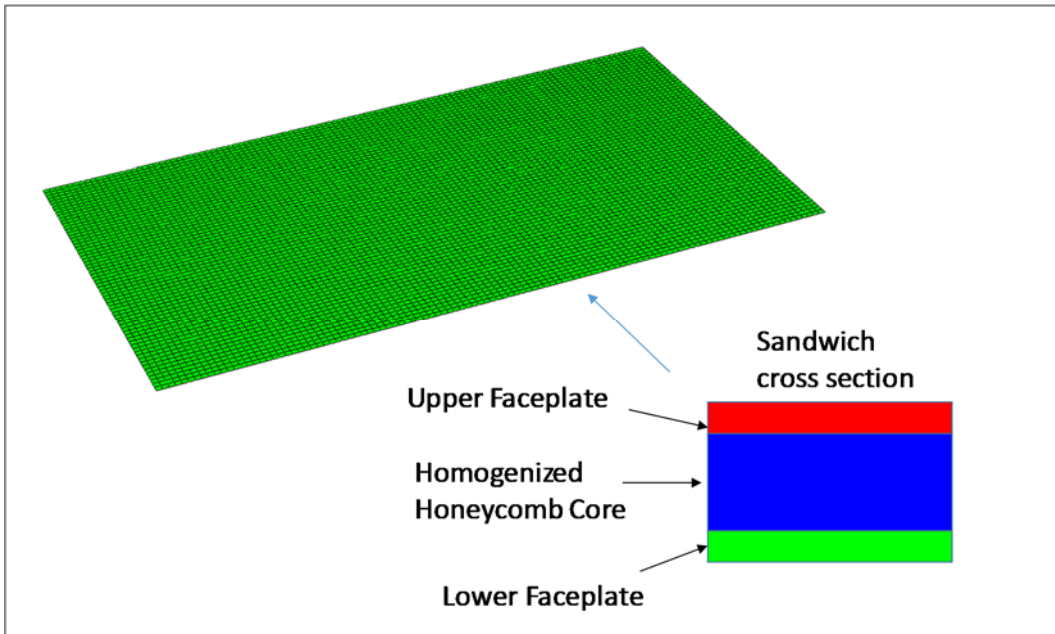


Figure 17. 2-D shell model with a homogenized core.

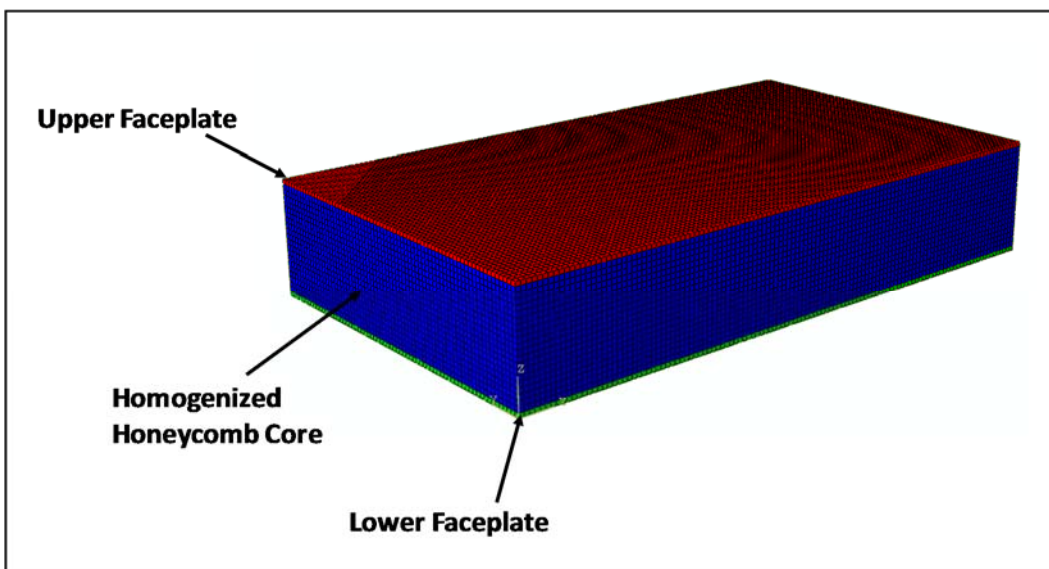


Figure 18. 3-D solid model with a homogenized core.

The homogenized 2-D shell model and 3-D solid models were analyzed using the same boundary conditions and loading used in the reference solution as depicted in Figure 16. The maximum displacements obtained using the homogenized core properties obtained for the three laminates described in Section 5 (Tables 9 to 12) are compared with the three reference solutions in the next section.

9. Comparison of maximum center deflection with reference solutions

This section completes the investigation into the coupled methodology to compute effective elastic properties of honeycomb cores with multi-layered walls. The reference problem selected in Section 7 represents a complex multi-cell model of a sandwich panel with realistic load conditions. The simplified FEM models developed in Section 8 contain homogenized representations of the central core and will necessarily contain various modeling aspects inherent to finite element simulations that may introduce differences in deflections predicted by the reference model and by the simplified homogenized models. Two sets of comparisons were made, one consisting of finite element predictions of deflections using FEM-derived effective moduli - which are considered the most accurate - and the second, consisting of finite element predictions using Gibson's approximations to the effective moduli of the core layer. It was assumed that the calculated deviations of the homogenized model deformations from the reference solution deformations represents inherent modeling differences between the different FEM representations, and the deviation of the same homogenized model using Gibson's effective moduli as the core material properties would yield a different percent deviation with the difference between the two due solely to the approximations inherent to Gibson's analytical method. It is shown in the following subsections that the difference between the homogenized models with the reference solutions is small, less than a maximum of 11.5%, but, more importantly, the difference between the homogenized models using effective FEM-derived core properties and Gibson's effective moduli were very small, less than two percent. This good agreement may be partly explained by the close agreement of the FEM-derived and the Gibson-derived effective modulus E_{zz} for the out-of-plane properties as shown in Tables 11 – 13.

9.1 Deflection comparison of a three-layered isotropic [Nomex/Nomex/Nomex] Laminate-1 core in a Sandwich plate with reference and homogenized solutions

The faceplates were assigned isotropic properties corresponding to a Nomex material with $E = 3150$ MPa, $\nu_{xy} = 0.4$ and $t = 0.25$ mm. Note that for Laminate-1, the homogenized effective core properties are the same using both CLT and the Chen-Chan equations due to the vanishing of the coupling matrix, B. The core in the homogenized model was assigned material properties from Table 12. The central deflections are listed in Table 18 where the percent deviation from the reference solution is also presented.

Table 18. Laminate-1 homogeneous model results compared to the reference model solution. The reference solution calculated a maximum center deflection of $\delta = -1.4758$ mm.

Homogeneous Models	Maximum deflection using effective moduli from FEM analysis	Deviation from reference solution	Maximum deflection using effective moduli from Gibson's equations	Deviation from reference solution
2-D Shell	-1.5660 mm	6.1%	-1.5672 mm	6.1%
3-D Solid	-1.5364 mm	4.1%	-1.5376 mm	4.2%

This analysis shows a good agreement between the simplified homogeneous models compared to the high-fidelity reference solution for approximating the behavior of the honeycomb core replaced by effective material properties. Comparing the maximum center deflection of the homogeneous models using FEM-derived and Gibson-derived effective core properties, the solutions are virtually identical, differing only by at most 0.1%

9.2 Deflection comparison of a symmetric three-layer isotropic [Al/Cu/Al] Laminate-2 core in a sandwich plate with reference and homogenized solutions

The faceplates were assigned steel properties with $E = 1.0E6$ MPa, $\nu_{xy} = 0.3$ and $t = 0.25$ mm. Note that for Laminate-2, the homogenized effective properties are the same using both the CLT and the Chen-Chan equations. The core in the homogenized model was assigned material properties from Table 13. The central deflections are listed in Table 19 where the percent deviation from the reference solution is also presented.

Table 19. Laminate-2 homogeneous model results compared to reference model solution. The reference solution calculated a maximum center deflection of $\delta = -.04594$ mm.

Homogeneous models	Maximum deflection using effective moduli from FEM analysis	Deviation from reference solution	Maximum deflection using effective moduli from Gibson's equations	Deviation from reference solution
2-D Shell	-.05065 mm	10.2%	-.05122 mm	11.5%
3-D Solid	-.04950 mm	7.74%	-.05007 mm	8.98%

This analysis shows a good agreement between the simplified homogeneous models compared to the high-fidelity reference solution for approximating the behavior of the honeycomb core replaced by effective material properties. The maximum percent difference is about 12 percent. Comparison of the maximum center deflection of the homogeneous models using FEM-derived and Gibson-derived effective core properties shows that the solutions are virtually identical, differing by at most 1.3%

9.3 Deflection comparison of a nonsymmetric three-layer isotropic [Al/Epoxy/Cu] Laminate-3 core in a sandwich plate with reference and homogenized solutions.

The faceplates were assigned Aluminum properties with $E = 70,300$ MPa, $\nu_{xy} = 0.33$ and $t = 0.25$ mm. For Laminate-3, the homogenized effective properties using CLT and the Chen-Chan

equations are different. Hence, both the homogenized properties obtained using CLT (Table 15) and obtained by Chen-Chan (Table 14) were analyzed and compared with the reference solution.

The central deflections obtained using Chen-Chan properties are compared with the corresponding center deflection from the reference in Table 20 where the deviation from the reference solution is also presented.

Table 20. Laminate-3 homogeneous model results using Chen-Chan effective wall modulus in Gibson's equations. The reference solution calculated a maximum center deflection of $\delta = -0.027685$ mm.

Homogeneous models	Maximum deflection using effective moduli from FEM analysis	Deviation from reference solution	Maximum deflection using effective moduli from Gibson's equations	Deviation from reference solution
2-D Shell	-0.028913 mm	4.4%	-0.028523 mm	3.9%
3-D Solid	-0.028327 mm	2.3%	-0.027921 mm	0.85%

Comparison of the maximum center deflection of the homogeneous models using FEM-derived and Gibson-derived effective core properties shows that the solutions are virtually identical, differing by at most 1.45%. The central deflections obtained using conventional CLT properties are compared with the corresponding center deflection from the reference solution, in Table 21.

Table 21. Increase in error of center deflection using CLT in Laminate-3 for the effective wall modulus in Gibson's equations. The reference solution calculated a center deflection $\delta = -0.027685$ mm.

Homogeneous Models	Maximum deflection using effective moduli from Gibson's equations	Deviation from reference solution
2-D Shell	-0.025772 mm	8.9%
3-D Solid	-0.028951 mm	4.6%

Results obtained using homogenized effective properties from the Chen-Chan equations result in more accurate predictions of the center deflection for Laminate-3, which consists of materials representative of electrodes and electrolyte that could be used in a battery.

10. Summary

The homogenization of complex core architectures is important to decrease the overall computational requirements in the simulation of multifunctional sandwich composites. This has a direct impact on the rapid assessment and optimization of design prototypes accounting for geometric sizing and material applications. A primary objective of this study was to investigate the accuracy of extending the widely used Gibson's approach to cellular structures with multi-layered walls that are designed for multifunctionality.

This work investigated a coupled approach using Chen-Chan's correction to classical lamination theory to compute equivalent moduli for multi-layered core-walls for use in the beam bending solutions of Gibson. The generality of this approach makes it extendable to wall configurations with an arbitrary number of layers. An equivalent wall modulus and the effective core properties can be calculated using a small set of closed-form analytical expressions. It was demonstrated that, as the width of the face plate separation increased, Gibson's 1-D elasticity solutions departed from the FEM simulation of the effective core moduli as the 2-D stress state became more pronounced and that a plate bending solution was more accurate in capturing the cell deformations. This departure, however, was shown to approach a bounded maximum value as the core width increased beyond a few multiples of the cell size. For the core widths examined, this maximum departure was 18% for the in-plane moduli, E_{xx} and E_{yy} .

For illustration, several multi-layered wall configurations were selected with differing material properties and symmetry across the midline. It was shown through comparison to unit cell finite element calculations that the analytically estimated equivalent core properties are obtained with good accuracy for the different multi-layered wall layers considered.

As a final test, a highly refined model of a 10 x 10 cell sandwich composite panel with all cells explicitly modeled was generated to serve as a reference solution to compare the accuracy of simplified FEM models incorporating homogenized cores. The panel was clamped along the edges and subjected to a normal pressure over the upper surface. A simplified 2-D shell element model and a 3-D solid element model were developed to simulate the sandwich panel with a homogenized core. For each model, two different simulations were performed and compared to the reference solution. One used FEM-derived equivalent moduli for the core – which are considered the most accurate – and one used the analytical moduli based on Gibson's approach. The difference in the maximum center deflection between the homogenized model with FEM-derived equivalent moduli and the reference solution were assumed to be based on various FEM modeling approximations inherent to the representation of the sandwich panel. The same deviation was calculated using effective core moduli obtained from Gibson's analysis. All these departures from the reference solution were reasonably small, the maximum being 11.5%. However, it was also shown that the difference between the homogenized models using FEM-derived or Gibson's effective moduli was within 2% for the three different laminated walls considered.

In conclusion, the coupled analytical solution for effective core moduli investigated in this study demonstrated an efficient method to simplify the modeling of multifunctional sandwich composite cores while maintaining a high accuracy compared to a computationally intensive explicit simulation of complex core configurations.

11. References

1. P. Liu, E. Sherma and A. Jacobsen, "Design and fabrication of multifunctional structural batteries," *J. Power Sources*, Vol. 189, pp. 646-650, 2009.
2. R.F. Gibson, "A review of recent research on mechanics of multifunctional composite materials and structures," *Comp. Struct.*, Vol. 92, pp. 2793-2810, 2010.
3. K.J. Narayana and R.G. Burela, "A review of recent research on multifunctional composite materials and structures with their applications," *Materials Today: Proceedings*, Vol. 5, pp. 5580-5590, 2018.
4. L.E. Asp and E.S. Greenhalgh, "Structural power composites," *Comp. Sci. Tech.*, Vol. 101, pp. 41-61, 2014.
5. P.L. Loyselle, "Multifunctional Structures for High Energy Lightweight Load-bearing Storage," NASA Glenn Research Center, <https://ntrs.nasa.gov> , Document ID 20180000928.
6. H.E. Soliman, "Mechanical properties of cellular core structures," Ph.D. Thesis, Virginia Polytechnic Institute and State University, March 21, 2016.
7. L. J. Gibson et al., "The mechanics of two-dimensional cellular materials," *Proc. R. Soc. Lond. A*, Vol. 382, pp. 25-42, 1982.
8. I.G. Masters and K.E. Evans, "Models for the elastic deformation of honeycombs," *Comp. Struct.* Vol. 35, pp. 403-422, 1996.
9. S. Malek and L. Gibson, "Effective elastic properties of periodic hexagonal honeycombs," *Mech. Mat.*, Vol. 91, pp. 226-140, 2015.
10. H.S. Moghaddam, C. Yang, S.R. Keshavanarayana, and A.L. Horner, "Analysis of in-plane mechanical response of hexagonal honeycomb core: Effect of node bond adhesive and proposed analytical method," *Proc. American Society for Composites*, 32nd Technical Conference, Oct. 23-25, 2017.
11. S.R.Keshavanarayana, H.Shahverdi, A.Kothare, C.Yang and J.Bingenheimer,"The effect of node bond adhesive fillet on uniaxial in-plane responses of hexagonal honeycomb core," *Comp. Struct.*, Vol. 175, pp. 111-122, 2017.
12. S. Sorohan, M. Sandu, D.M. Constantinescu, and A.G. Sandu, "On the evaluation of mechanical properties of honeycombs by using finite element analysis," *INCAS Bulletin*, Vol. 7, pp. 135-150, 2015.
13. M. Hajianmaleki and M.S. Qatu, "Mechanics of composite beams," Ch22 *Advances in Composite Materials – Analysis of Natural and Man-Made Materials*, Ed. P. Tesinova, IntechOpen, 2011.
14. R.M. Jones, *Mechanics of Composite Materials*, Hemisphere Publishing Corp., 1975.
15. D. J. Chen and W.S. Chan, "Use of composite effective moduli for lumping layers in finite element analysis," American Institute for Aeronautics and Astronautics paper AIAA-96-1568-CP, 1996.
16. Abaqus Analysis User's Guide. 2018. Abaqus 2018, DS Simulia Corp., Providence, RI, USA.
17. F.E. Penado, "Effective elastic properties of honeycomb core with fiber-reinforced composite cells," *Open J. Comp. Mater.*, Vol. 3, pp. 89-96, 2013.

18. M. Tauhiduzzaman and L.A. Carlsson, "Influence of constraints on the effective in-plane extensional properties of honeycomb core," *Comp. Struct.*, Vol. 209, pp. 616-624, 2019.
19. J. Hohe and W. Becker, "A refined analysis of the effective elasticity tensor for general cellular sandwich cores," *Int. J. Solids Struct.*, Vol. 38, pp. 3689-3717, 2001.

REPORT DOCUMENTATION PAGE

Form Approved
OMB No. 0704-0188

The public reporting burden for this collection of information is estimated to average 1 hour per response, including the time for reviewing instructions, searching existing data sources, gathering and maintaining the data needed, and completing and reviewing the collection of information. Send comments regarding this burden estimate or any other aspect of this collection of information, including suggestions for reducing the burden, to Department of Defense, Washington Headquarters Services, Directorate for Information Operations and Reports (0704-0188), 1215 Jefferson Davis Highway, Suite 1204, Arlington, VA 22202-4302. Respondents should be aware that notwithstanding any other provision of law, no person shall be subject to any penalty for failing to comply with a collection of information if it does not display a currently valid OMB control number.
PLEASE DO NOT RETURN YOUR FORM TO THE ABOVE ADDRESS.

1. REPORT DATE (DD-MM-YYYY) 1-04-2019		2. REPORT TYPE Technical Memorandum		3. DATES COVERED (From - To)	
4. TITLE AND SUBTITLE An Analytical Method to Calculate Effective Elastic Properties of General Multifunctional Honeycomb Cores in Sandwich Composites				5a. CONTRACT NUMBER	
				5b. GRANT NUMBER	
				5c. PROGRAM ELEMENT NUMBER	
6. AUTHOR(S) Saether, Erik; Krishnamurthy, Thiagarajan				5d. PROJECT NUMBER	
				5e. TASK NUMBER	
				5f. WORK UNIT NUMBER 975105.09.23	
7. PERFORMING ORGANIZATION NAME(S) AND ADDRESS(ES) NASA Langley Research Center Hampton, VA 23681-2199				8. PERFORMING ORGANIZATION REPORT NUMBER L-21020	
9. SPONSORING/MONITORING AGENCY NAME(S) AND ADDRESS(ES) National Aeronautics and Space Administration Washington, DC 20546-0001				10. SPONSOR/MONITOR'S ACRONYM(S) NASA	
				11. SPONSOR/MONITOR'S REPORT NUMBER(S) NASA-TM-2019-220275	
12. DISTRIBUTION/AVAILABILITY STATEMENT Unclassified- Subject Category 24 Availability: NASA STI Program (757) 864-9658					
13. SUPPLEMENTARY NOTES					
14. ABSTRACT Sandwich composite structures are ideal configurations in which to incorporate additional functionality beyond load carrying capabilities. The inner core-walls can be layered to incorporate other functions such as power storage for a battery. In this work we investigate an assemblage of analytical tools to compute effective properties that allow complex layered core architectures to be homogenized into a single continuum layer. This provides a great increase in computational efficiency to numerically simulate the structural response of multifunctional sandwich structures under applied loads. We present a coupled analytical method including an extensive numerical verification of the accuracy of this method.					
15. SUBJECT TERMS Effective moduli; Honeycomb core; Sandwich composites					
16. SECURITY CLASSIFICATION OF:			17. LIMITATION OF ABSTRACT	18. NUMBER OF PAGES	19a. NAME OF RESPONSIBLE PERSON
a. REPORT	b. ABSTRACT	c. THIS PAGE			STI Help Desk (email: help@sti.nasa.gov)
U	U	U	UU	35	19b. TELEPHONE NUMBER (Include area code) (757) 864-9658